Influence of spin structures and nesting on Fermi surface and a pseudogap anisotropy in t-t'-U Hubbard model.

A.A.Ovchinnikov and M.Ya.Ovchinnikova.

Institute of Chemical Physics, RAS, Moscow, 119977, Kosygin str., 4.

Abstract

Influence of two types of spin structures on the form of the Fermi surface (FS) and a photoemission intensity map is studied for t - t' - U Hubbard model. Mean field calculations are done for the stripe phase and for the spiral spin structure. It is shown, that unlike a case of electron doping, the hole-doped models are unstable with respect to formation of such structures. The pseudogap anisotropies are different for h- and e- doping. In accordance with ARPES data for $La_{2-x}Sr_xCuO_4$ the stripe phases are characterized by quasi-one-dimensional segments of FS in the vicinity of points $M(\pm \pi, 0)$ and by suppression of spectral weight in diagonal direction $k_x = k_y$. It is shown that spiral structures display the polarisation anisotropy: different segments of FS correspond to electrons with different spin polarisation.

PACS: 71.10.Fd, 74.20.Rp, 74.20.-z

The angular resolved photoemission spectroscopy (ARPES) is effective in the study of electronic structure of cuprates [1, 2]. It gives the image of the Fermi surface (FS) projection onto a CuO_2 plane. Conclusions of the early works (see [1, 2], and references therein) were consistent with FS of the hole type centered at point $Y(\pi,\pi)$ of two-dimensional Brillouin zone (BZ). Later other versions of the FS topology have been discussed. In particular, a presence of an electron type of the FS have been proposed with the center at $\Gamma(0,0)$ in $Bi_2Sr_2CaCu_2O_{8+\delta}$ (BSCCO) [3]. Revision of the problem [4, 5] partly confirms the original version. At the same time for $La_{2-x}Sr_xCuO_2$ (LSCO) it has been proved a transition from h-type of the FS to e-type during transition from underdoped (UD) to overdoped (OD) regions of the phase diagram [6, 7]. The ARPES data gave an evidence of the d-wave superconducting gap and of the opening of the pseudogap (PG) in

UD BSCCO. Recently a bilayer splitting of bands [8, 9, 10, 11] in BSCCO and the time reversal symmetry breaking in UD BSCCO [12] have been discovered.

A wide use of the photoemission intensity maps in the space k_x, k_y, ω poses a problem of extracting the FS from the ARPES data. One aspect of the problem, calculation of the matrix elements is discussed in [13, 14]. However the FS topology and intensities of various (main or shadow) segments of the FS depend also on the spin and charge structures of a ground state of a system.

The goal of the present work is a model study of the influence of periodic structures on the FS and the photoemission intensity based on the t-t'-U Hubbard model. Unlike the static structures in manganites, in cuprates one deals with rather dynamical structures with a time scale larger than time $t > 10^{-6} \div 10^{-9}$ sec in the μ -SR experiments. So at small times or for the processes with energy resolution higher than \hbar/t the local spin structures may be considered in quasi-static limit. Then the question arises about a correspondence of the structures to the ARPES data. The experimental indications of the SDW and CDW structures in cuprates are the incommensurate peaks in the spin susceptibility at $q = (\pi \pm \delta q, \pi), (\pi, \pi \pm \delta q)$ in LSCO [15], linear structures along the CuO_2 bonds with period 4a (a is a lattice constant) observed in the tunnel spectra [16], periodic chess structure $4a \times 4a$ around the vortex in mixed state of BSCCO [17] etc.

Here we study the stripe and spiral structures in the simplest mean field (MF) approach, interpret the PG, discuss examples of structures with the different types of the PG anisotropy and to connect some properties of MF solutions with features observed in some cuprates. Earlier [18] the DDW (d- density wave) structure has been proposed as a possible hidden order parameter (OP) in cuprates. Here a search of possible OP is extended to stripe and spiral structures. Stabilization of such structures originates from the removing of a degeneracy of states in "hot points" - the van Hove singularities (VHS) or in parallel segments of the FS at the so-called nesting.

Consider a t-t'-U Hubbard model with the zero band energies

$$\epsilon_k = 2t(\cos k_x + \cos k_y) + 4t'\cos k_x \cos k_y \tag{1}$$

Further we put t = 1, so all energies are measured in units of t. In MF approximation this Hamiltonian is insufficient to describe the superconducting (SC) pairing. It may be supplemented by an empirical pairing interaction of electrons at neighboring centers deduced in more accurate approaches (for example, [19]). But here we study a normal

state and therefore retain the original t - t' - U model.

A periodic 2D structure is determined by two translation vectors

$$E_1 = (E_{1x}, E_{1y}), \quad E_2 = (E_{2x}, E_{2y})$$
 (2)

and the corresponding vectors of the inverse lattice B_1, B_2 which satisfy the relations $E_i B_j = 2\pi \delta_{ij}$. (The components of E_i B_i are in units of the corresponding constants of the original and inverse lattices). The unit cell of the structure contains n_c sites with coordinates $j = (j_x, j_y)$, so that each site $n = n(L, j) = (n_1, n_2) = E_1 L_1 + E_2 L_2 + (j_x, j_y)$ is determined by the integers L_1, L_2 determining the position of the unit cell and by integers $j = (j_x, j_y)$, fixing the site inside the unit cell.

Let \tilde{k} is the quasi-momentum inside the main BZ \tilde{G} of a given periodic structure unlike the momentum k from the BZ G of the original lattice. The areas of \tilde{G} and G are restricted by conditions $|\tilde{k}B_i| \leq \pi$ or $|k_{x(y)}| \leq \pi$. The order parameters of the periodic structures are the mean charges and spin densities on sites of the unit cell

$$r_j = \frac{1}{N_L} \sum_L \langle r_{n(L,j)} \rangle; \quad S_{\mu j} = \frac{1}{N_L} \sum_L \langle S_{\mu,n(L,j)} \rangle$$
 (3)

Here μ numerates the spin components, $N_L = N/n_c$ is a number of the unit cells, n_c is a number of sites in it. In the MF approximation the mean energy (1) is $\overline{H} = \langle T \rangle + N_L U \sum_j (r_j^2 - \sum_\mu S_{j\mu}^2)$ and the wave function is determined by the occupation of the one-electron eigenstates $\chi_{k\lambda}^{\dagger}$ of the linearized Hamiltonian

$$H_{lin} = T + N_L \sum_{j} \{2Ur_j \hat{r}_j - 2US_{\mu j} \hat{S}_{\mu j}\} = \sum_{\tilde{k} \in \tilde{G}} \hat{h}_{\tilde{k}}.$$

The latter is divided into independent contributions from each reduced quasi-momentum \tilde{k} . Here \hat{r}_j , $\hat{S}_{\mu j}$ are the operators corresponding to averages (3). In the momentum representation the eigenstates of $\hat{h}_{\tilde{k}}$ are expanded over a basis set of $2n_c$ Fermi operators

$$\chi_{\tilde{k}\lambda}^{\dagger} = \sum_{m,\sigma} c_{\tilde{k}+Bm,\sigma}^{\dagger} W_{m\sigma,\lambda}(\tilde{k}), \tag{4}$$

where $\lambda = 1, ..., 2n_c$, $Bm = B_1m_1 + B_2m_2$ and $m = (m_1, m_2)$ is such set of integers, that allows the vectors $\tilde{k} + Bm$ to share all phase space G.

The matrix of eigenvectors $W_{m\sigma,\lambda}$ and the eigenvalues $E_{\tilde{k},\lambda}$ are determined by diagonalization of $h_{\tilde{k}}$ in the basis set $\{c_{\tilde{k}+Bm,\sigma}^{\dagger}\}$:

$$(h_{\tilde{k}})_{m\sigma,m',\sigma'}W_{m'\sigma',\lambda} = W_{m\sigma,\lambda}E_{\tilde{k},\lambda}$$

$$(5)$$

Here

$$(h_{\tilde{k}})_{m\sigma,m',\sigma'} = \delta_{mm'}\delta_{\sigma\sigma'}\epsilon_{\tilde{k}+Bm} + U\sum_{j}\varphi(j,m'-m)[r_{j}\delta_{\sigma\sigma'} - S_{\mu j}(\sigma_{\mu})_{\sigma\sigma'}]$$
 (6)

with $\varphi(j,m) = \exp[i(j-j_0)Bm]$; $Bm = B_1m_1 + B_2m_2$. In turn, the order parameters (3) are expressed as

$$\{r_j, S_{\mu j}\} = \frac{1}{2N} \sum_{\tilde{k} \in \tilde{G}} \sum_{ms, m's'} \{\sigma_0, \sigma_\mu\}_{ss'} \varphi(j, m' - m) W_{ms, \lambda}^*(\tilde{k}) W_{m's', \lambda}(\tilde{k}) f(E_{\tilde{k}\lambda} - \mu)$$
 (7)

Here the Puali matrices σ_{μ} , σ_0 in (9) correspond to the components $S_{\mu j}$, r_j and f is the Fermi function. Equations (9) determine the self-consistent MF solution.

The intensity of the photoemission of electron with a projection k of the momentum on ab plane and the energy $E = h\nu - \omega$ is

$$I(k,\omega) = |M(k)|^2 A(k\omega) f(\omega) \otimes R_{\omega k}. \tag{8}$$

It is determined by the matrix element M(k), a spectral density $A(k\omega)$ and the Fermi function f. Usual convolution is done with the Gaussian function $R_{\omega k}$ [13] with parameters, which characterize a finite resolution over k and energy. The dependence of the matrix element M on k was studied in [13, 14]. Here for simplicity we take a constant value for it, since we study an effect of the structure on the spectral density A. In the one-electron approximation

$$A(k,\omega) = \frac{1}{N} \sum_{\tilde{k} \in \tilde{G}} \sum_{m,\sigma,\lambda} |W_{m\sigma,\lambda}(\tilde{k})|^2 \overline{\delta}(E_{\tilde{k}\lambda} - \mu - \omega) \delta_{k,\tilde{k}+Bm}$$
(9)

Here $\lambda=1,\ldots,2n_c$ and index $m=(m_1,m_2)$ numerates all independent Umklapp vectors $Bm=B_1m_2+B_2m_2$. A standard replacement of the δ - function in (9) by a function with finite width Ω is implied. A map of $I(k_x,k_y,\omega=0)$ allows to visualize both the main and shadow segments of the FS. Though the band energies are periodic functions in k space ($E_{\tilde{k}+Bm,\lambda}=E_{\tilde{k},\lambda}$ for any $m=(m_1,m_2)$), the intensity (8) does not posses such periodicity. Therefore even for the constant matrix element M in (8) various segments of the FS display themselves with a different intensity due to the Umklapp processes in the case of SDW or CDW structure.

The intensity map allows easily to repeat the known results [20, 21, 22, 23, 24, 25, 26] about changing of the FS topology with increase of the doping and opening the pseudogap

in UD region for the homogeneous AF solutions. The energies of the lower and upper Hubbard bands are

$$\epsilon_{\tilde{k}\lambda} = 4t'\cos k_x \cos k_y \pm \sqrt{U^2 d_0^2 + 4t^2(\cos k_x + \cos k_y)^2} + const \tag{10}$$

The VHS in the DOS of the lower band correspond to the "hot points" $M = (\pm \pi, 0), (0, \pm \pi)$. A form of the FS critically depends on a sign of t'. At t' = 0 energy $E_{\lambda}(k)$ is constant for all k along the magnetic Brillouin zone (MBZ) boundary. At t' > 0 the energies at the points M are lower than at the diagonal points. This leads to the formation of the known hole pockets around points $(\pi/2, \pi/2)$ or the electron pockets around $(\pi, 0), (0, \pi)$ in UD case of the h- or e- doped models [21]. In the same UD region the PG is open at x, y directions or at diagonal directions for h- or e- doped models. Such a topology is determined by a profile of the energies $E_{\lambda}(k)$ of lower or upper Hubbard bands as a function of k on the MBZ boundary. But this profiles are greatly influenced also by a formation of the spin or charge structures in system.

The MF calculations allow to test a stability or an instability of the homogeneous AF states with respect to the formation of the periodic spin or charge structures. The Fig.1 presents the mean energy $\overline{H} = \langle H \rangle$ as a function of doping $\delta = |1-n|$ for the normal state of the hole- and electron- doped models for a set of structures. In addition to homogeneous paramagnet (PM) and AF solutions the next structures are considered:

- 1) The stripe structure which consists of the antiphase AF stripes parallel to the y-axis. A fixed width 4a of the stripe (8 sites in a unit cell of the structure) is taken and the domain walls are chosen as centered on bonds or on the sites. Both structures have a similar form of the FS, but that with the bond-centered domain walls occurs to have some lower energy and only it is discussed below.
 - 2) The spiral spin structures

$$\langle S_n \rangle = d_0[\mathbf{e}_x \cos Qn + \mathbf{e}_y \sin Qn]$$
 (11)

with spirality vector $Q = Q_x = \pi(\eta, 1)$ or $Q = Q_{xy} = \pi(\eta, \eta)$, with $\eta \sim 0.75 - 0.8$.

- 3) The checkered structure with antiphase AF square domain $4a \times 4a$. It have a higher energy than the above two structures, and unrealistic shape of the FS, so the results are not presented here.
- 4) The proposed in [18] states of the orbital antiferromagnet with staggered currents on a plackets. In MF approximation they do not appear for t t' U Hubbard model

without additional interactions. At hole doping and $U/t \ge 5$ there exist the MF solutions with staggered spin currents and rotations on $\pi/2$ of local spins of the neighbor sites. But their energies are higher than those of stripe and spiral structures and corresponding results are not presented here.

Most of calculations were carried out for structures with fixed commensurate period 8a, though the optimal size of the AF domains or spiral vector depend on doping. For spiral states the dependence of $Q(\delta)$ has been calculated many times. Here we are interested only in the specific features of the FS and the pseudogap anisotropy.

Fig. 2 shows that at the h-doping the homogeneous AF solutions are unstable with respect to formation of the stripe and spiral structures. Formation of these structures extend the doping range where the local spin retains a nonzero value (a disappearing of the $\langle S_{\mu j} \rangle$ corresponds to matching of the energy of some structure and that of the paramagnet state). At the same time at e-doping the MF energies of the above structures appear to be higher than the energy of the homogeneous AF solution. Large stability of the AF state in the e-doped models corresponds to the more wide region of the AF order in cuprates of the n-type than in ones of the p-type. The result about the absence of the stripe and spiral structures in the n-type models are consistent also with a commensurate peak at $Q \sim (\pi, \pi)$ in the spin susceptibility observed in NCCO, PCCO (unlike the incommensurate peaks in the hole doped cuprates).

Fig.2a presents a map of the intensity $I(k, \omega = 0)$, Eqs.(8,9), for the stripe structure in the model with U/t = 6, t'/t = 0.1 at n = 0.8. In case of AF MF solution the chosen doping is close to the "optimal" doping at which the Fermi level passes through the VHS in the DOS of the lower Hubbard band. The stripes (which are parallel to an y-axis) split the VHS. The "hot points" $M_x = (\pi, 0)$ and $M_y = (0, \pi)$ become non-equivalent points and the quasi-1D asymmetric horizontal segments of the FS are formed. Fig.2b presents the intensity map symmetrized over the structures with the x- or y- stripe orientation. The FS form differs strongly from that for the homogeneous AF state of the model with t' > 0. The main difference is the absence of the FS in the diagonal direction and near the M_y . This gives an evidence that the stripes open the pseudogap in these regions of k. The corresponding band energies $E_{\lambda}(k)$ descend below the Fermi level and the work function $\Delta_{PG} = \mu - E_{\lambda} > 0$ for the electron to be removed from such k is observed as the PG in ARPES data. The revealed anisotropy of the FS and pseudogap may change our

conclusions about possible symmetry of the SC order in the striped state. The retaining of the quasi-1D segments of the FS only suggests the 1D character of conductivity along the stripe direction (here y-axis). With the increase of t' up to the value 0.3 there appear the small additional hole pockets at around $k_S = (\pi/2, \pi/2)$ in the intensity map.

The anisotropy of the FS and the PG suggests the revision of the possible symmetries of SC order coexisting with the stripes. If the structure is symmetric with respect to replacement $x \leftrightarrow y$, then the d-wave SC order $\langle c_{k\uparrow}^{\dagger} c_{-k\downarrow}^{\dagger} \rangle \sim \cos k_x - \cos k_y$ is expected. It provides the orthogonality of the pair function to the on-site pair function $c_{n\uparrow}^{\dagger} c_{n\downarrow}^{\dagger}$ which is suppressed by the on-site repulsion U. Taking into account a new FS view (see Fib.2a) one may suppose the extended s-wave SC pair function $\langle c_{k\uparrow}^{\dagger} c_{-k,\downarrow}^{\dagger} \rangle \sim \cos k_x + \cos k_y$. The latter might be orthogonal to the on-site pair function due to the node lines $k_x \pm k_y = \pm \pi$. Unlike the gain of the node lines in the angular dependence of the d-SC gap, one can suppose a gain of the node in an analogue of a "radial" part of the pair function. Verification of such hypothesis requires further calculations.

Fig.3a presents the one-electron energies $E_{\lambda}(k)$ (eigenvalues of MF problem) as functions of quasi-momentum varying along the contour

$$Y(-\pi,\pi) - M_y(0,\pi) - Y(\pi,\pi) - M_x(\pi,0) - Y(\pi,-\pi).$$

As expected, band energies $E_{\lambda}(k)$ are periodic functions with the period $\pi/4$ on the first horizontal segment of contour $Y - M_y - Y$. However, the intensity map selects only the energy levels which are non-shadow at given k. Fig.3b presents such map of $I(k,\omega)$ on the plane k,ω for k varying along the same contour. Intersections of band energies with the Fermi level in the vicinity of M_x correspond to quasi-1D FS of Fig.2a.

The above pictures may be explained by an action of the spin-dependent average field. The main harmonic of this field is $F(n) \sim \cos\{Q_{\eta}n + \varphi_0\}$ with $Q_{\eta} = (\eta \pi, \pi)$ (here $\eta = 0.75$). This field shifts upstairs the zero level $\epsilon(0, \pi)$ at M_y pushing it from the lower levels ϵ_k at $k = (\pm \eta \pi, 0)$ near M_x . The same field descends downstairs (lower the Fermi level) the zero level $\epsilon(\pi, 0)$ at M_x pushing it from the higher zero levels $\epsilon(\pm 0.25\pi, \pi)$ near M_y .

The ARPES data for UD LSCO [6, 7, 27] are in qualitative agreement with the properties of the model calculations. It was shown [6, 7, 27] a presence of two different segments of the FS - near the points M and at diagonal directions, systematic suppression of spectral weight near $(\pi/2, \pi/2)$ in comparison with BSCCO or OD LSCO, the straight segments of

the FS near $(\pi, 0)$ with the width $\sim \pi/2$. All these observed features have been interpreted as an evidence of nonhomogeneous stripe structures in UD LSCO [6, 7, 27] or the combine action of the stripe structure and of the order-disorder [28]. Our calculations confirm this interpretation. Another evidence of the stripe structure is given by the observation of the "incommensurate" peaks in neutron scattering at $k = (\pi \pm \delta, \pi), (\pi, \pi \pm \delta)$ in LSCO [15].

Another type of the spin and angular anisotropy of the FS manifests itself in spiral spin structures (11) which possess the polarisational anisotropy of the FS. Different segments of the FS correspond to the electrons with different preferential spin polarisation. Really, the average field from spiral spin structure mixes one-electron states $\{c_{k,\uparrow}^{\dagger}, c_{k+Q,\downarrow}^{\dagger}\}$ provides a splitting of the VHS's. But unlike the stripe structures, the occupations $n_{k,\sigma} = \langle c_{k\sigma}^{\dagger} c_{k\sigma} \rangle$ and intensities $I_{\sigma}(k\omega)$ of the photoemission of the electrons with fixed polarisation σ depends on this polarisation σ . Values $I_{\sigma}(k\omega)$ are determined by Eqs.(8,9), but without summing over σ in right part of (9).

Fig.4a presents a map of the intensity $I_{\sigma=\uparrow}(k,\omega=0)$ for the spiral state with $Q=(0.8\pi,\pi)$ and for the spin polarisation $\sigma=\uparrow$ on the axis z normal to the plane of the spin rotation of the spiral structure (11). Thus a photoemission of electrons with the up spin polarization ($\sigma=\uparrow$) corresponds to the strongly anisotropic FS. For the opposite spin polarisation the FS coincides with the FS of Fig.3a, reflected in the plane x=0. Fig.3b presents the FS, symmetrized over the spins and over two types of structures with $Q=(0.8\pi,\pi)$ $Q=(\pi,0.8\pi)$. In the vicinity of the point M the FS have both the intersection with the line M-Y typical for the FS of the h-type and the same with the line $M-\Gamma$ typical for the e-type of the FS. Such double intersections have been probably observed in ARPES data of BSCCO [1, 2]. Direct comparison with experiment would require to take into account the bilayer structure of BSCCO and the corresponding band splitting.

Polarisational anisotropy of the FS directly reflects the existence of the spin currents $J_{\uparrow} = -J_{\downarrow}$ in the spiral state. According to [29] it might be a reason of the time reversal symmetry breaking observed in the UD BSCCO in dichroism of the ARPES signal [12]. In the alternative hypothesis [12, 30] this effect is explained by the specific alignment of the circular micro currents.

A direct observation of the polarisational anisotropy of the FS needs the selective over the spin polarisation measurements of the photoemission intensity. Such selective measurements of the total photoemission have been achieved in the so called "spin-orbit" photoemission [31]. In principle, similar selectivity is possible in ARPES also. It is important to continue the study of the time reversal symmetry breaking, in particular, to clarify, whether this effect and accompanying currents have the surface or bulk character. Yet we cannot answer the question: if the ground state of the BSCCO might be presented as a set of quasi-static domains with the spiral structure and corresponding systems of spin currents.

In conclusion, the MF treatment of the normal state of the t-t'-U Hubbard model shows that the FS topology and the PG anisotropy depends on sign of t', on the type (e- or h-) of the doping and of the spin structure. For the hole-doped models the homogeneous AF MF state occurs to be unstable with respect to formation of the stripe phase and the spiral spin structure. However, in electron-doped models the lowest energy refers to the homogeneous AF solution. This corresponds to a wide doping range of an existence of the local AF order in the n-type cuprates NCCO, PCCO and to commensurate peak at $Q=(\pi,\pi)$ observed in neutron scattering in these cuprates. In accordance with the ARPES data for the LSCO, the stripe phase is characterized by the quasi-1D behavior of the FS in the vicinity of the "hot points" $(\pm \pi,0)$, by the pseudogap opening and by suppression of the spectral weight in the diagonal direction and in the direction parallel to stripes. Such anisotropy of FS and PG does not conform with the d- symmetry of the SC order. For the spiral spin structure the polarisation anisotropy of FS is revealed which means that different segments of the FS correspond to different spin electron polarisations.

Work is supported by the Russian Foundation of Basic Research under Grant No.03-03-32141. Authors are greatfull to V.Ya.Krivnov for stimulating discussions.

Fig.1.

In the top fig. the doping dependencies of the mean energy (per one site) for the hole doped t - t' - U model with parameters U = 4.0, t' = 0.3 for different spin structures are shown: for the paramagnet state (curve PM), for the homogeneous AF state (curve AF), for the stripe phase with a period of 8a along the x-axis (dashed line 1), for the spiral states with vectors $Q = \pi(\eta, 1)$ (curve 2) and $Q = \pi(\eta, \eta)$ (curve 3) at $\eta = 0.8$. The bottom graphics- the energies of the same structures (with the same notations) for the electron-doped model. For convenience the common function $F(\delta) = U(n^2 - 1)$ is subtructed from all energies.

Fig.2.

a. A map of the photoemission intensity $I(k, \omega = 0)$ for the antiphase AF stripes parallel to the y axis, having a width 4a and the bond-centered domain walls. b. The same, but averaged over two stripe phases of x- and y- orientation. Parameters of model are U = 6, t' = 0.1.

Fig.3.

a. The eigenenergies $E_{\lambda}(k)$ of the MF problem as functions of the quasi-momentum running along the contour $Y(-\pi,\pi)$ - $M_y(0,\pi)$ - $Y(\pi,\pi)$ - $M_x(\pi,0)$ - $Y(\pi,-\pi)$ for the stripe structure with period 8a along the x-axis. b. The map of the intensity $I(k,\omega)$ for k, running along the same contour. The map displays the same levels $E_{\lambda}(k)$, but with a spectral weight, determined by the structure of band states. Parameters of the model are the same, as in Fig.2.

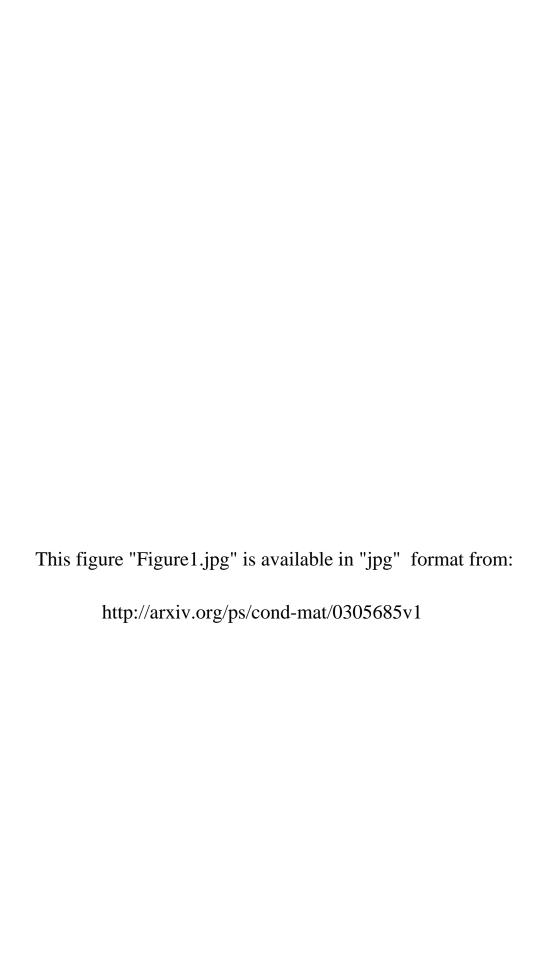
Fig.4.

a. The map of the photoemission intensity $I_{\uparrow}(k,\omega=0)$ for the electrons with a spin polarisatin $\sigma=\uparrow$ for the spiral structure with $Q=\pi(0.8,1)$. b. The same but averaged over two spin polarisations $\sigma=\uparrow,\downarrow$ and over two structures with $Q=(0.8\pi,\pi)$ and $(\pi,0.8\pi)$. The model parameters are U=6, t'=0.1.

References

- A.Damascelli, Z.-X.Shen, Z.Hussain, Rev.Mod.Phys., 75, 473, (2003); cond-mat/0208504.
- [2] Z.M.Shen, D.S.Dessau, Phys.Rep., 253, 1 (1995)
- [3] Y.-D.Chuang, A.D.Gromko, D.S.Dessau, Y.Aiura, Y.Yamaguchi, K.Oka, A.J.Arko, J.Joyce, H.Eisaki, S.I.Uchida, K.Nakamura, Y.Ypichi, Phys.Rev.Lett. **3717** (2000).
- [4] H.M.Fretwell, A.Kaminski, J.Mesot, et al., Phys.Rev.Lett. 84, 4449 (2000).
- [5] S.V.Borisenko, M.S.Golden, S.Legner, et al., Phys.Rev.Lett. 84, 4453,(2000).
- [6] A.Ino, C.Kim, T.Mizokawa, et al., J.Phys.Soc.Jpn. 68 1496 (1999).
- [7] T, Yoshida, X.J.Zhou, M.Nakamura, S.A.Kellar, et al., cond-mat/0011172
- [8] D.L.Feng, N.P.Armitage, D.H.Lu, et al., Phys.Rev.Lett., 86, 5550 (2000).
- [9] Y.D.Chuang, A.D.Gromko, A.Fedorov, et al., Phys.Rev.Lett. 87, 117002 (2001).
- [10] A.A.Kordyuk, S.V.Borisenko, T.K.Kim, et al., cond-mat/0110379; Phys.Rev.Lett., 89, 077003 (2002).
- [11] A.Kamiski, S.Rosenkranz, H.M.Fretwell, et al. cond-mat/0210531
- [12] A.Kaminsky, S.Rosenkranz, H.M. Fretwell, et al., cond-mat/0203133
- [13] S.V.Borisenko, A.A.Kordyuk, S.Legner, et al., Phys.Rev.B **64**, 094513 (2001).
- [14] A.Bansil and M.Lindroos, Phys.Rev.Lett, 5154 (1999); M.Lindroos, S.Sahrakorpi and A.Bansil, Phys.Rev.B65, 054514 (2002).
- [15] R.J.Birgeneau, G.Shirane in Physical Proprties of High Temperature Superconductors. I. Ed.D.M.Ginzberg, World Scientific, Singapoore, 1989.
- [16] C.Howald, H.Eisaki, N.Kaneko, A.Kapitulnik, cond-mat/0201546; Phys.Rev.B 67, 014533, (2003).
- [17] J.E.Hoffman, E.A.Hudson, K.M.Lang, et al., Science, 295, 466, (2002)

- [18] S.Chakravarty, R.B.Laughlin, D.K.Morr, Ch.Nayak, E-print archiv cond-mat/0005443; Phys.Rev.B **63**, 094503 (2001).
- [19] A.A.Ovchinnikov and M.Ya.Ovchinnikova, Zhur. Eksp. Teor. Fiz. 110, 342 (1996); 112 (1997) 1409.
- [20] N.M.Plakida, V.S.Oudovenko, R.Horsch, and A.J.Liechtenstein, Phys.Rev. B55, 11997 (1997).
- [21] A.A.Ovchinnikov, M.Ya.Ovchinnikova, Phys.Lett.
 A249, 531 (1998). A.A.Ovchinnikov, M.Ya.Ovchinnikova and E.A.Plekhanov, Pisma Zhur.Eksp.Teor.Fiz. 67, 350 (1998); Zhur.Eksp.Teor.Fiz. 114, 985 (1998); 115, 649 (1999).
- [22] R.O.Kuzian, R.Hayn, A.F.Barabanov, and L.A.Maksimov, Phys.Rev. B 58, 6194 (1998).
- [23] F.Onufrieva, P.Pfeuty, and M.Kisilev, Phys.Rev.Lett B 82, 2370 (1999).
- [24] A.A.Ovchinnikov and M.Ya.Ovchinnikova, Zhur.Eksp.Teor.Fiz. 118, 1434, (1999)
- [25] C.Kusko, R.S.Markiewicz Phys.Rev.Lett., 84, 963 (2000)
- [26] C.Kusko, R.S.Markiewicz, M.Lindroos and A.Bansil cond-mat/0201117; Phys.Rev.B 66,14051, (2002).
- [27] A.Ino, C.Kim, M.Nakamura, et al., Phys.Rev. **B62**, 4137 (2000).
- [28] X.J.Zhou, T.Yoshida, S.A.Kellar et al. Phys.Rev.Lett. 86, 5578, (2001).
- [29] M.Ya.Ovchinnikova, Zhur.Eksp.Teor.Fiz. in press (2003); A.A.Ovchinnikov and M.Ya.Ovchinnikova, cond-mat/0210632
- [30] C.M.Varma, Phys.Rev.Lett., 83, 3538 (1999).
- [31] G.Ghiringhelli, L.H.Tjeng, A.Tanaka et al. Phys.Rev.B 66, 75101 (2002).



This figure "Figure2.jpg" is available in "jpg" format from: http://arxiv.org/ps/cond-mat/0305685v1

